Physical Sciences Section

FAR ULTRAVIOLET ELECTRONIC SPECTRA OF SrF$_2$ AND BaF$_2$

Mohammad Nisar and Mme Simone Robin

Laboratoire de Spectroscopie, Université de Rennes, Avenue du Général Leclerc, 35031 Rennes-Cedex, France

Abstract. Reflectance measurements at 20° incidence are carried out on *in situ* cleaved single crystals of SrF$_2$ and BaF$_2$ at room temperature in the energy range 8–35 eV. A method of Kramers–Kronig is applied for the determination of optical constants and other useful functions. Interband transitions are identified at Γ, X and L points with the aid of a recently calculated band structure. Two plasmons are identified for each of the two fluorides.

Resume. Des mesures de pouvoir réflecteur sous une incidence de 20° sont faites dans le domaine de 8–35 eV sur des monocristaux de SrF$_2$ et BaF$_2$ clivés sous vide, à la témperature ambiante. Les constantes optiques et autres fonctions usuelles sont calculées par la methode de Kramers–Kronig. Des transitions interbandes sont identifiées aux points Γ, X et L à l'aide d'un schéma de bandes récemment calculé. Deux plasmons sont mis en évidence pour chacun des deux fluorures.

Fluorite type crystals (CaF$_2$, SrF$_2$, BaF$_2$) have a large electronic forbidden gap and their fundamental absorption is found to be in the vacuum ultraviolet. Experimental work in this region presents various difficulties, mainly a suitable radiation source that could provide an intense continuum enabling thus to study thoroughly the rich spectra of these fluorides. In recent years, extensive experimental work has been carried out on these substances, thanks to the improved techniques in this spectral region. Stephan *et al.*[1] studied the optical properties of CaF$_2$ in the energy range 10–45 eV, Tomiki and Miyata[2] carried out the reflectivity measurements between 9–13.5 eV (at 78° ≤ T ≤ 573°K) and calculated ε_1 and ε_2, Hayes *et al.*[3] give the reflectivity curves of these crystals between 10–30 eV and interpret their results in the light of computer-calculated excitation energies for different configurations in free metallic ions. Rubloff[4] gives a detailed account of reflectivity measurements on these fluorides and other ionic crystals in the energy range 6–36 eV. In a recent paper, Frandon *et al.*[5] report their characteristic energy-loss measurements on thin films in the energy range 8–40 eV. The results reported in references 4 and 5 have been interpreted on the basis of assumed band structures at points Γ and X. Starostin *et al.*[6] reported recently their band structure calculations at Γ, X and L points for these fluorides but unfortunately the conduction band calculations are incomplete. The lack of complete band structure calculations renders the task of interpretations quite delicate and difficult.

Experimental Techniques

We have investigated the optical properties of single crystals of SrF$_2$ and BaF$_2$ in the energy range 8–35 eV. The details of the apparatus and the experimental techniques are described elsewhere.[7] The single crystals, procured from the Harshaw Chemical Company, were cleaved in a vacuum of about 10^{-5} torr and were studied without being exposed to air. For a first sample of freshly cleaved BaF$_2$ crystal, we observed a considerable amount of fluorescent light. The intensity of the fluorescent light on other specimens of ultraviolet quality (UVQ) was found to be of rapidly decreasing nature with the aging of the cleaved surface. Specimens cleaved in air did not show any fluorescent light. The UVQ specimens cleaved in vacuum were left in the experimental chamber for sometime and reflectance measurements at 20° incidence were carried out when almost no fluorescent light was observable. A method of Kramers–Kronig transformation is then applied for the determination of the optical constants and other useful functions.

The resonance absorption of high energy photons by the ionic insulators is related to three types of interactions, namely electron–hole interaction giving rise to excitonic peaks, electron–crystal potential interaction responsible for the interband transitions and finally the electron–electron interaction giving rise to plasmons. Different structures on our curves will be interpreted from the point of view of these three types of interactions.

Results and Interpretations

Figures 1 and 2 show the reflectance spectra of SrF$_2$ and BaF$_2$, Figs. 3 and 4, the optical constants n and k, Figs. 5 and 6 real and the imaginary parts of the complex dielectric constant while the energy-loss functions are shown in Figs. 7 and 8. The agreement is good on the whole with the recent results but some structures are shifted by a few eV. R$_{20}$° and ε_2 curves are divided into two distinct regions: 10–20 eV and 20–35 eV for SrF$_2$ and 10–18 eV and 18–35 eV for

BaF$_2$; the first zone corresponds to the excitations of valence electrons, the second to core electrons.

The first two band schemes proposed by Onodera[8] and Rubloff[4] differ essentially for the minimum of the conduction band at Γ or X points. The recent band structure calculations carried out by Starostin (Figs. 9, 10) show the minimum of the conduction band at Γ point. This calculated band scheme helps to precise the origin of a few transitions between 10–15 eV for the two fluorides. The positions of different observed structures are summarized in Table 1. The excitations of valence band electrons towards the conduction band give rise to excitonic peaks in the region 10–15 eV but their origin should be carefully attributed to the different symmetry points of the Brillouin zone.

The peaks A at 10.4 and 10 eV respectively on the ε$_2$ curves of SrF$_2$ and BaF$_2$ are due to the transition L$_3$L$_3'$→L$_1$. Starostin et al.[6] calculate them at 10.8 and 10 eV respectively. We think that the structure B at 12.1 eV on ε$_2$ curve of SrF$_2$ is due to the transition
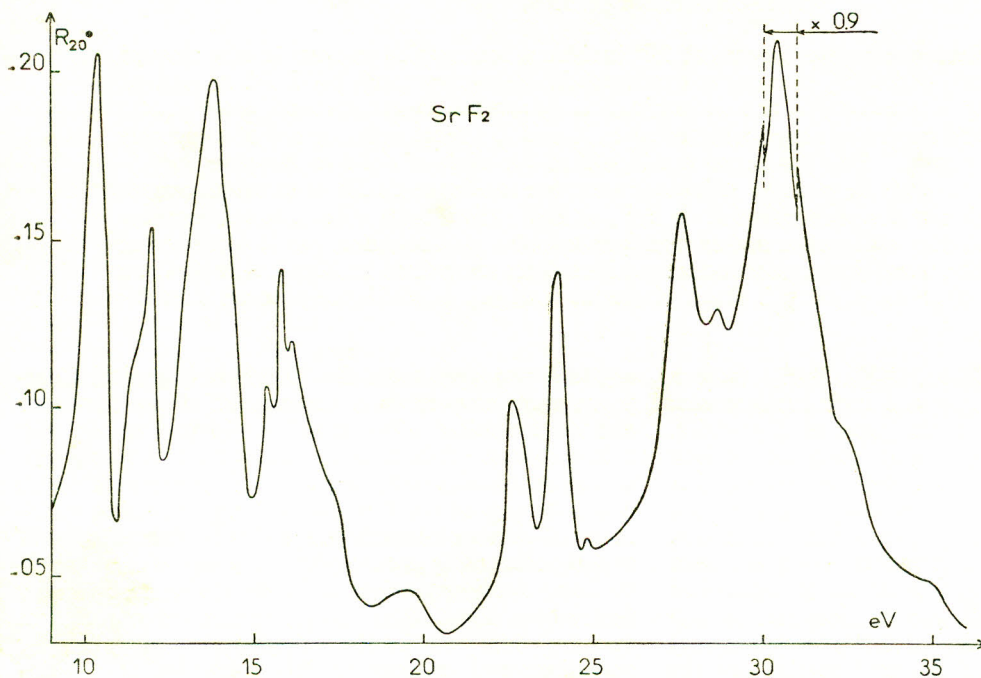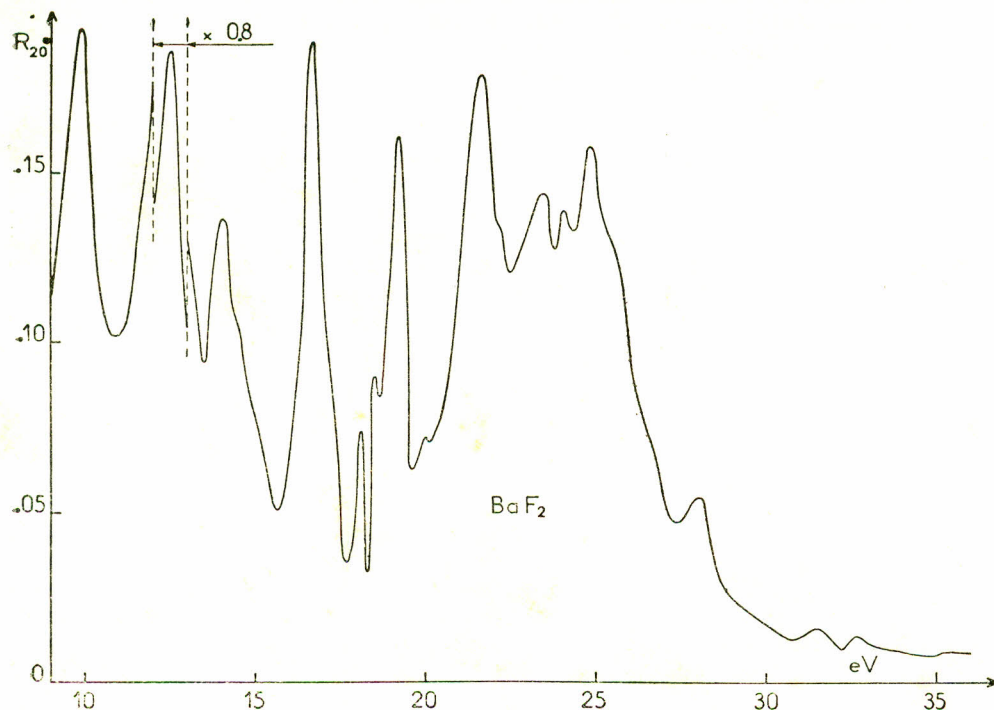

Fig. 1. Reflectance curve for SrF$_2$.

Fig. 2. Reflectance curve for BaF$_2$.

$X_5' \rightarrow X_3$. The structures C at 13.8 eV in the case of SrF₂ and 12.5 eV in the case of BaF₂ are identified due to $X_5' \rightarrow X_I$ transition. The calculated values[6] happen to be exactly the same. $\Gamma_{15} \rightarrow \Gamma_I$ transition in the case of SrF₂ is identified at D (14.2 eV) and the corresponding transition in BaF₂ is found to occur at B (11.7 eV). The calculated values[6] for $\Gamma_{15} \rightarrow \Gamma_I$ transitions in SrF₂ and BaF₂ are 14.2 and 11.9 eV respectively. Then, in the case of SrF₂, we observe an important structure F at 15.8 eV on ε_2 curve surrounded by two small peaks E (at 15.4 eV) and G (at 16.1 eV). We assign it to the transition $\Gamma_{15} \rightarrow \Gamma_{25}'$. The corresponding transitions in the case of BaF₂ are expected to be at lower energies than in SrF₂; the structure D at 14.1 eV in BaF₂ is identified due to the

transition $\Gamma_{15} \rightarrow_{25}'$. Structures H and F at 17.5 eV and 16.7 eV on SrF₂ and BaF₂ curves respectively can be attributed to $\Gamma_{15} \rightarrow \Gamma_{12}$ transitions. The limit of the valence band excitation is nearly 20 eV for SrF₂ and 18 eV for BaF₂. Strong structures are observed again towards higher energy region where core band excitations occur. We suppose that (4p)Sr⁺⁺ and (5p)Ba⁺⁺ core bands are flat; as the minimum of the conduction band is situated at point Γ, the energies for the transitions occuring at Γ points should be less than those at points X. The structures L (at 23 eV) and M (at 24 eV) on ε_2 curve of SrF₂ and the structures K (at 19.2) and M (at 21.7) on ε_2 curve of BaF₂ are assigned to $\Gamma_8^- \rightarrow \Gamma_I$ and $\Gamma_6^- \rightarrow \Gamma_I$ transitions respectively. The calculated spin-orbit splitting of p-core bands in
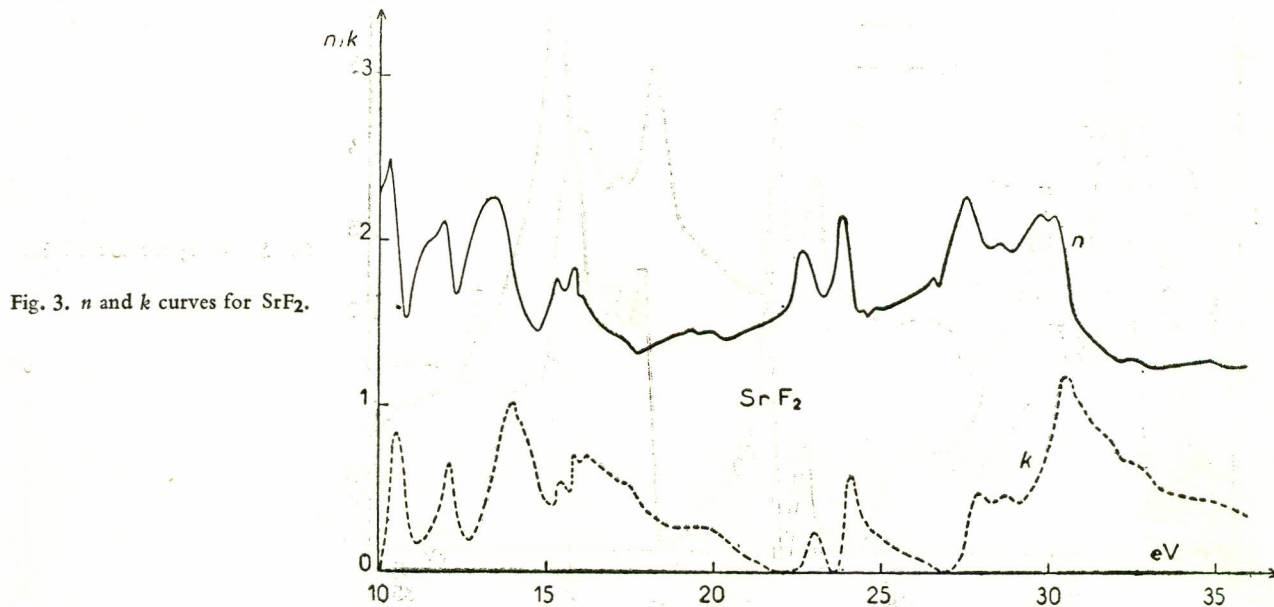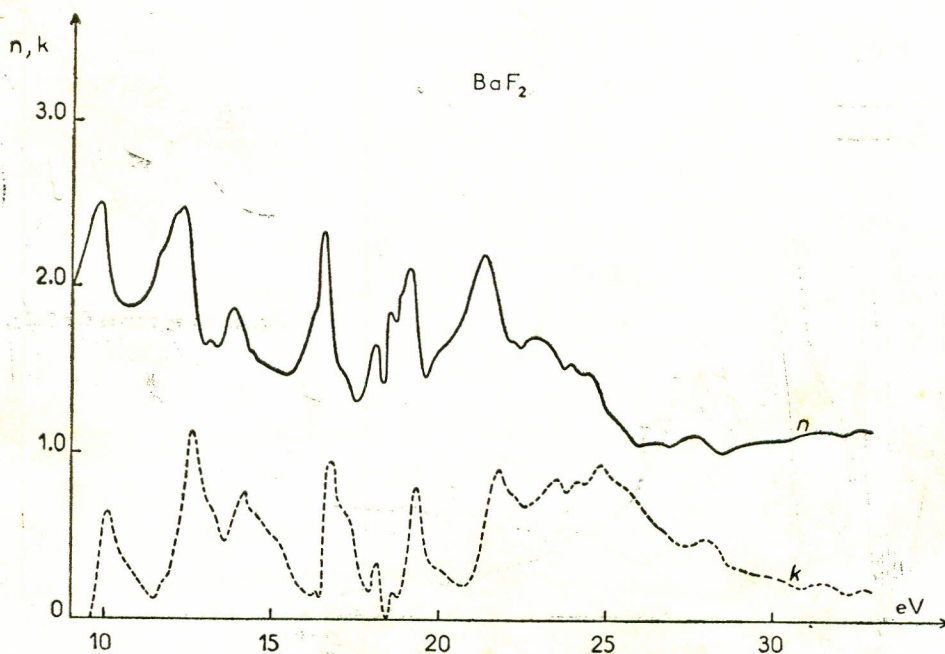

Fig. 3. n and k curves for SrF₂.

Fig. 4. n and k curves for BaF₂.

SrF_2 and BaF_2 are 1.1 and 2 eV respectively.[3] Experimentally the pairs of structures (L,M) and (K,M) are separated by 1 and 2.5 eV; it is, therefore, reasonable to attribute these structures due to the spin-orbit splitting of the p-core bands.

We identify the structures P (at 27.9 eV) and Q (at 28.7 eV) of SrF_2 and the two structures L and N at 20.0 and 22.2 eV of BaF_2 to be $(X_7^- \rightarrow X_3)$ and $(X_6^- \rightarrow X_3)$ core excitons. The structures S at 30.4 eV in SrF_2 and X at 28.0 eV in the case of BaF_2 are attributed to Sr^{++} $(4p) \rightarrow$ conduction band and Ba^{++} $(5p) \rightarrow$ conduction band transitions respectively. The structure T

at 32.4 eV in the case of SrF_2 it most probably due to F^- $(2s) \rightarrow$ conduction band transition.

It has been shown experimentally that two plasmons are generally observed in the ionic crystals.[4,7] The first plasmon is found in the valence band excitation region while the second in the core band excitation region. Moreover, the frequencies of these plasmons can be calculated by applying Horie's formula:

$$\omega_p^2 = \omega_g^2 + (Ne^2/m\varepsilon_0)$$

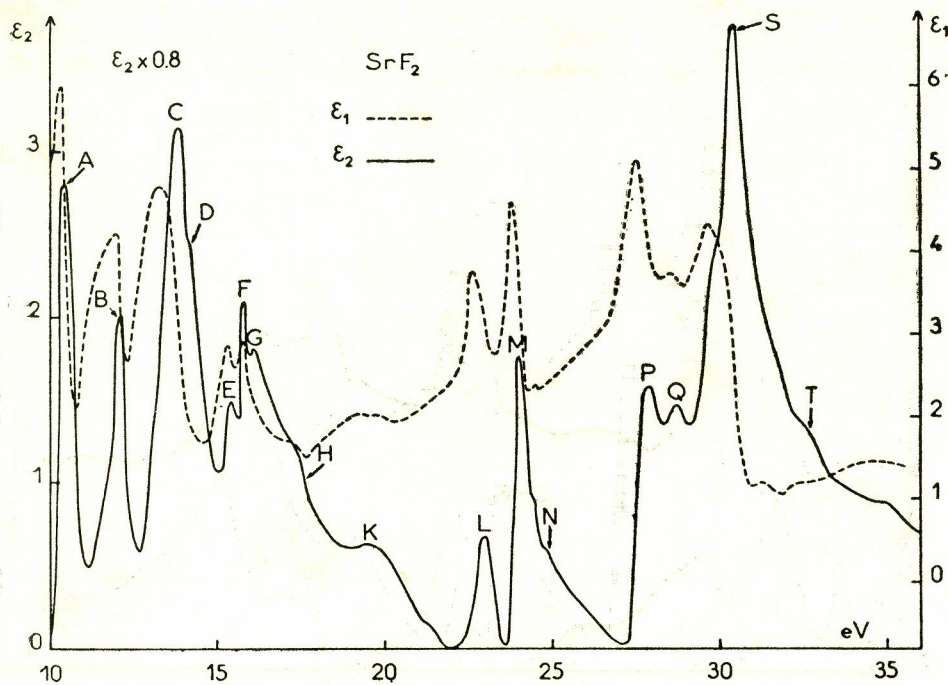ωg being the band width. The exact widths of the forbidden gaps in these crystals are unknown. However,

Fig. 5. ε_1, ε_2 curves for SrF_2.

Fig. 6. ε_1, ε_2 curves for BaF_2.
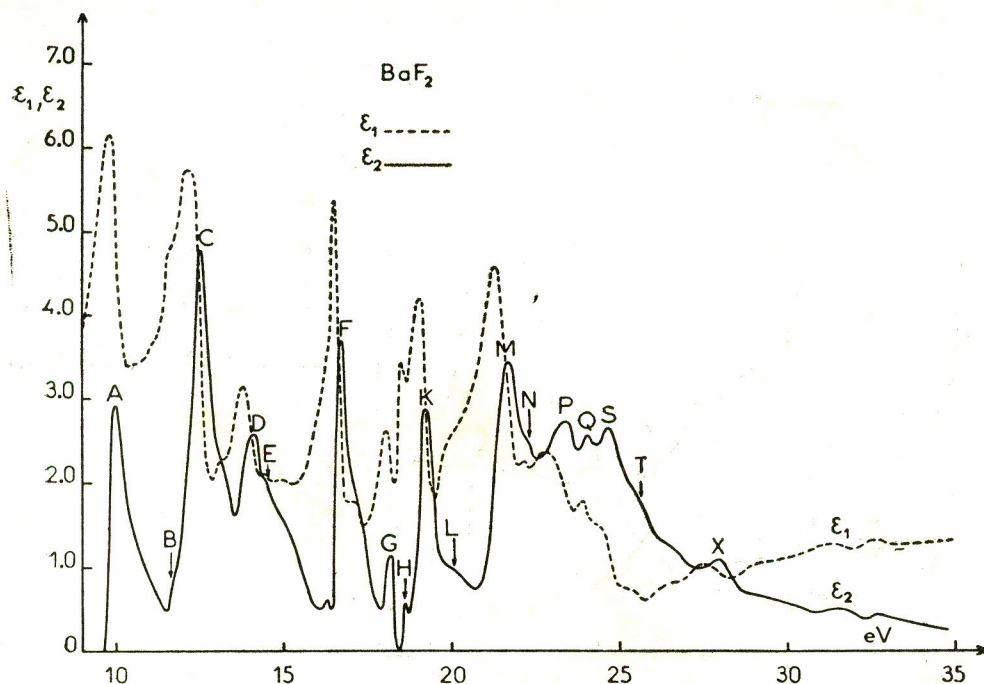
Kalder *et al.*9 give an estimated width of 10.8 eV in SrF₂. For SrF₂, our energy-loss function shows a maximum at 17.6 eV and the corresponding curve of Frandon *et al.*. peaks at 17.2 eV. This structure can be assigned to the plasmon of valence electrons. Now if we assume 22 electrons of SrF₂ 'molecule' taking part in the collective resonance phenomenon, the Horie's formula gives 27.8 eV for the energy of the plasmon. Our experimental value is 32.2 eV.

The existence of a plasmon of valence electrons at 17.4 eV in BaF₂ is quite probable. In fact the values of ε_I and ε_2 are small and the corresponding curves are ascending and descending respectively around this position. For the $5p$ electrons of Ba^{++} the plasmon is situated experimentally at 26.5 eV while the Horie's formula, with $\hbar\omega_g = 11$ eV, gives 25.1 eV. In the two cases, the arrangement is reasonably good if one takes into account the simplicity of the applied for-

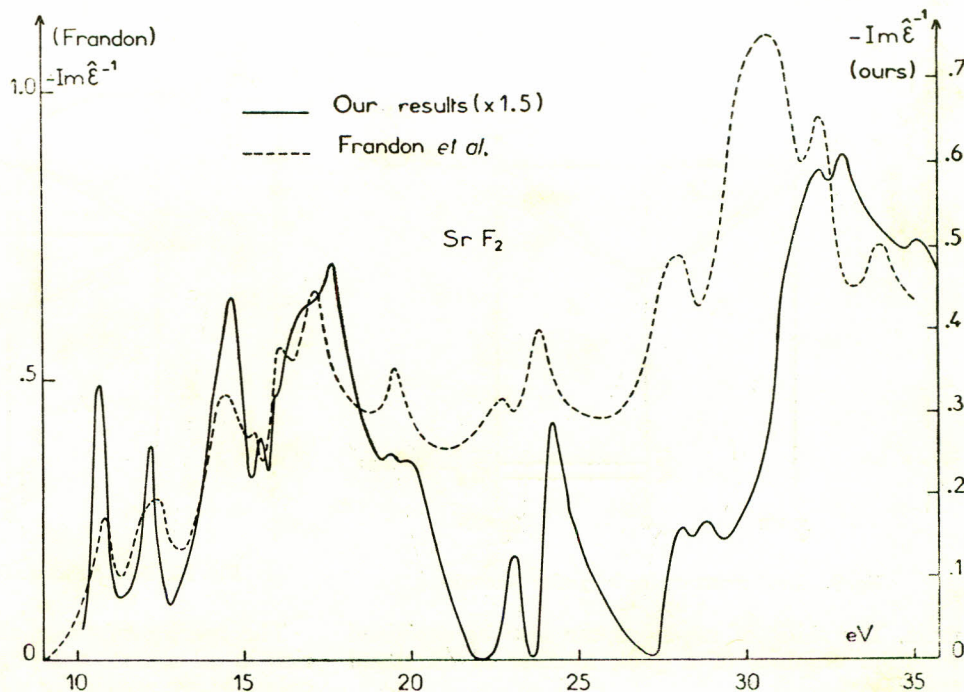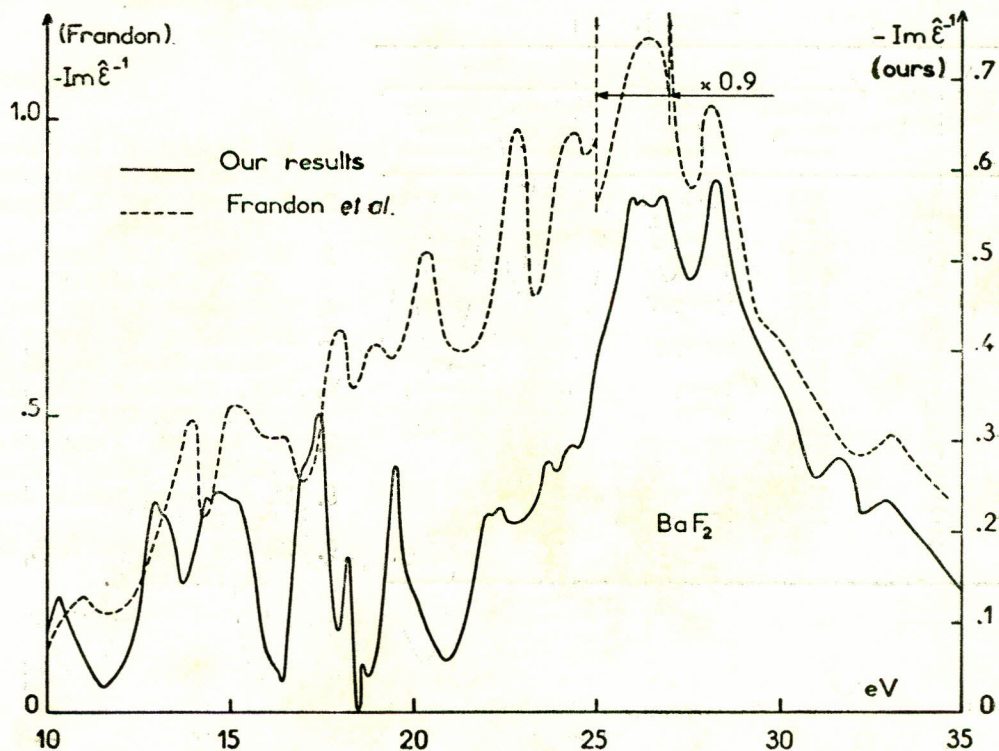
Fig. 7. Energy loss function curve for SrF₂.

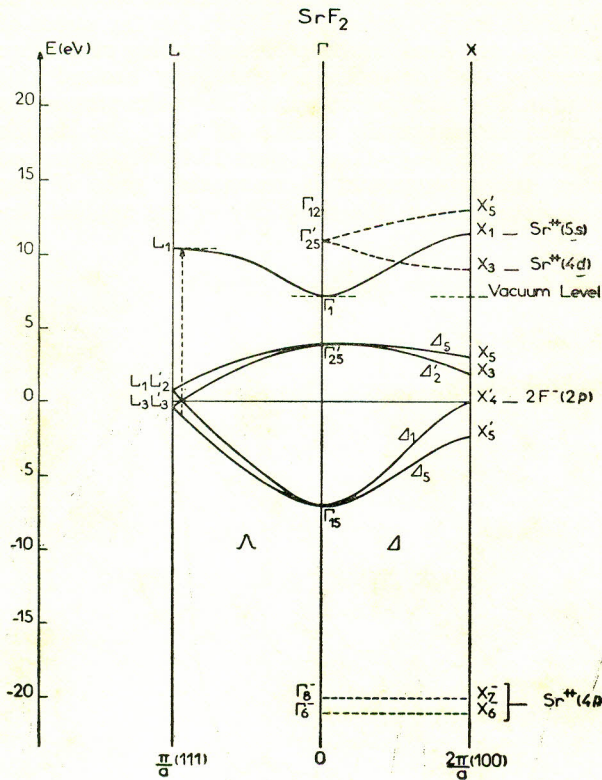Fig. 8. Energy loss function curve for BaF₂.

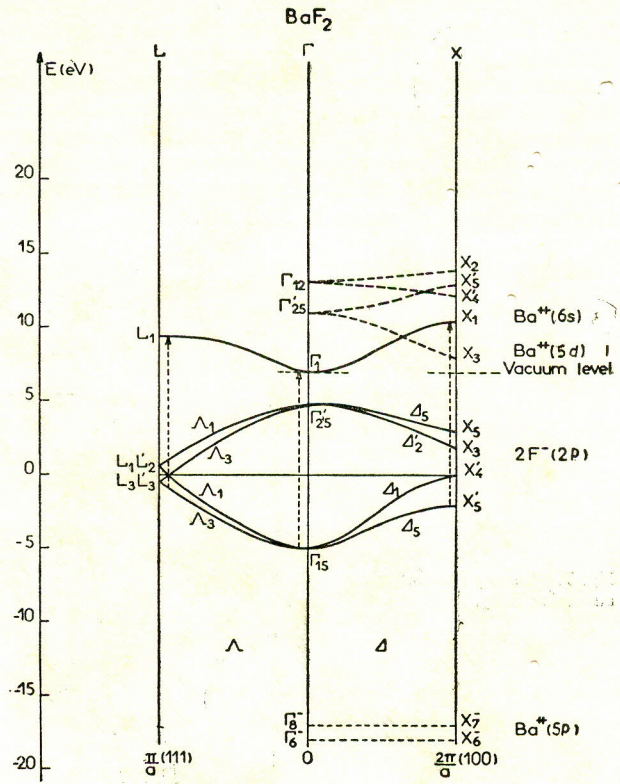Fig. 9. Band structure for SrF$_2$ after Starostin

Fig. 10. Band structure for BaF$_2$ after Starostin.

mula. The shifts of plasmons can also be explained with the vicinities of a great number of interband transitions.

The spectra of these alkaline earth fluorides are rich in all aspects and complete band structure calculations are needed for a better understanding of the observed structures.

TABLE 1.

Designation of peaks	SrF$_2$		BaF$_2$	
	Positions on ε_2 curve	Possible interpretations	Positions on ε_2 curve	Possible interpretations
A	10.4	$L_3L'_3 \to L_1$	10.0	$L_3X'_5 \to \gamma_1$
B	12.1	$X'_5 \to X_3$	11.7	$\gamma_{15} \to \gamma_1$
C	13.8	$X'_5 \to X_3$	12.5	$X_5 \to X_1$
D	14.2	$\gamma_{15} \to \gamma_1$	14.1	$\gamma_{15} \to \gamma_{25}$
E	15.4		14.5	
F	15.8	$\gamma_{15} \to \gamma_{25}'$	15.7	$\gamma_{15} \to \gamma_{12}$
G	16.1		18.2	
H	17.5	$\gamma_{15} \to \gamma_{12}$	18.6	
K	19.5		19.2	$\gamma_8 \to \gamma_1$
L	23.0	$\gamma_8 \to \gamma_1$	20.0	$X_7 \to X_3$
M	24.0	$\gamma_6 \to \gamma_1$	21.7	$\gamma_6 \to \gamma_1$
N	24.8		22.2	$X_6 \to X_3$
P	27.9	$X_7^- \to X_3$	23.4	
Q	28.7	$X_6^- \to X_3$	24.0	
S	30.4	$Sr^{++}(4p) \to$ C.B.	24.7	
T	32.4	$F^-(2s) \to$ C.B.	25.5	
X			28.0	$Ba^{++}(5p) \to$ C.B.

References

1. G. Stephan, Y. Le Calvez, J.C. Lemonnier and S. Robin, J. Phys. Chem. Solids, **30,** 601 (1969).
2. T. Tomiki and T. Miyata, J. Phys. Soc. (Japan), **27,** 658 (1969).
3. W. Hayes, A.B. Kunz and E.E. Koch, J. Phys., C, **4,** L200 (1971).
4. G.W. Rubloff, Phys. Rev. B, **5,** 662 (1972).
5. J. Frandon, B. Lahaye and F. Pradal, Physica Status Solidi (b), **53,** 565 (1972).
6. N.V. Starostin, T.E. Chebotareva and V.K. Zakharov, Opt. Spectr. **33,** 141 (1972).
7. G. Stephan, These détat (1970) Faculte des Sciences, Rennes, France.
8. Y. Onodera, private communication, cited in ref. 2.
9. K.A. Kalder and A.F. Malysheva, Opt. Spectr. **31,** 135 (1971).